Recent Advances in Cyanobacterial Biotransformations

Lenny Malihan-Yap[1], Hanna C. Grimm[1], and Robert Kourist[1,2,*]

DOI: 10.1002/cite.202200077

Light-driven biotransformations in recombinant cyanobacteria have been explored in recent years for the production of chiral compounds and platform chemicals. In particular, cyanobacteria harboring oxidoreductases proved to be sustainable hosts providing and recycling reducing equivalents and improving the atom economy of the reactions. However, the provision of light in photobioreactors is considered to be the major bottleneck for up-scaling. In this review, genetic tools for generating recombinant cyanobacterial strains and up to date cyanobacterial biotransformations including redesigning of the photosynthetic electron transport chain to increase specific activities are presented. Finally, several photobioreactor geometries to circumvent the light limitation are discussed and some future perspectives are presented.

Keywords: Biocatalysis, Biotransformations, Cyanobacteria, Photosynthesis

Received: May 25, 2022; *revised:* June 30, 2022; *accepted:* August 05, 2022

1 Introduction

In the last decade, the interdisciplinary field of photobiocatalysis received considerable attention because of the attractive possibility to use light as energy source for biochemical transformations. Different approaches are presented in literature: (1) the application of photoenzymes, (2) enzyme-photocatalyst-coupled systems (EPCS), and (3) light-driven biotransformation (Fig. 1) [1, 2]. Photoenzymes are photobiocatalysts in the true sense of the word as they employ light-dependent mechanisms. While they offer highly interesting reactions, only three photoenzymes have been discovered so far: (1) photolyases [3], (2) light-dependent protochlorophyllide reductases (LPORs) [4], and (3) fatty acid photodecarboxylases (FAP) [5–7]. EPCS combine chemical photocatalysts with enzymes. The diverse reactivities of photocatalysts and the often outstanding selectivity of enzymes give rise to highly interesting one-pot multistep reactions. [8] EPCS are also often considered for the recycling of redox cofactors, where photosensitizer directly or indirectly provides photoexcited electrons for enzymatic redox reaction and resulting electron holes in the valence band are filled by sacrificial electron donor molecules such as organic compounds with tertiary amine functionality. [1, 8] The current state of the art in the application of photoenzymes and EPCS is summarized in several excellent reviews. [1, 2, 8, 9]

Light-driven biotransformation uses phototrophic organisms like microalgae [10, 11] or cyanobacteria as host for enzymatic reactions. Required reduction equivalents, such as nicotinamide adenine dinucleotide phosphate (NADPH) or reduced ferredoxin (Fd), are regenerated via oxygenic photosynthesis, which presents an atom-efficient cofactor recycling system that does not require the addition of sacrificial co-substrates. Fig. 2 shows the representative photosynthetic machinery found in the thylakoid membrane. During photosynthesis, light is absorbed in photosystem II (PSII), which induces the water splitting reaction, and the released electrons are transported across the thylakoid membrane to regenerate the reaction equivalents. During electron transport, protons are pumped to the luminal side of the thylakoid membrane generating an electrochemical gradient that drives adenosine triphosphate (ATP) production. NADPH and ATP are required for downstream metabolic processes such as the Calvin-Benson-Bassam (CBB) cycle that fixes carbon dioxide. Reduced Fd is a central hub for the distribution of electrons to different pathways and electron sinks [12]. Especially cyanobacteria have emerged as promising whole-cell biocatalysts owing to their fivefold higher photosynthetic activity as compared to terrestrial plants, their faster growth rate, and their inedible nature which does not compete for food resources [13–15]. Moreover, cyanobacteria are more amenable to genetic modification than algae.

Wild-type cyanobacteria have been investigated for classical whole-cell biotransformations over the last four

[1]Dr. Lenny Malihan-Yap, Hanna C. Grimm,
Prof. Dr. Robert Kourist
kourist@tugraz.at
Graz University of Technology, Institute of Molecular Biotechnology, NAWI Graz, 8010 Graz, Austria.
[2]Prof. Dr. Robert Kourist
ACIB GmbH, 8010 Graz, Austria.

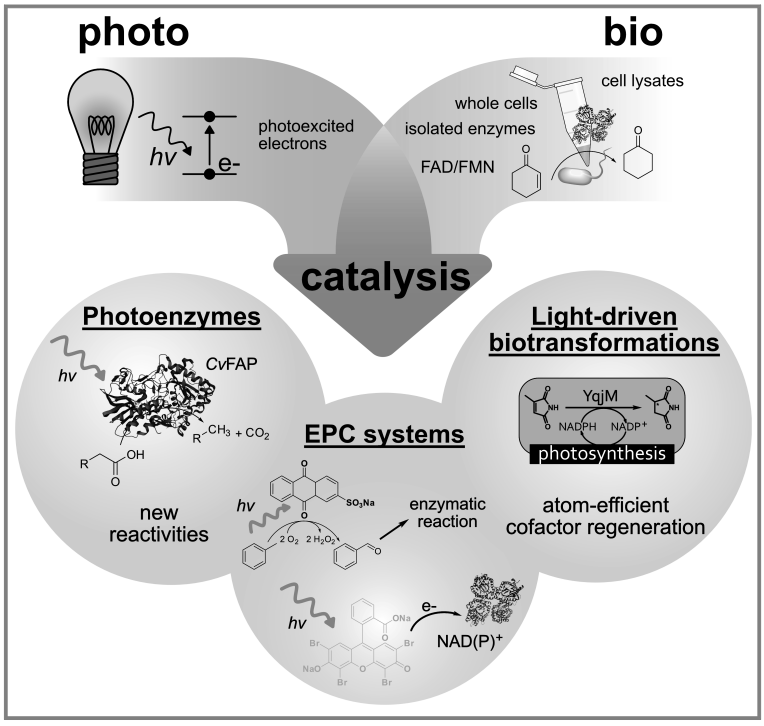

Figure 1. The interdisciplinary field of photobiocatalysis combines biocatalysts with light as energy source. While photoenzymes directly convert light energy into chemical energy, enzyme-photocatalyst-coupled systems (EPCS) mimic photosynthesis by using light energy to provide electrons for chemical transformations. Light-driven biotransformations in whole cells exploit natural photosynthesis for atom-efficient cofactor recycling [1].

decades [16]. In 2016, we showed that recombinant production of a bacterial ene-reductase in *Synechocystis* sp. PCC 6803 (from now on *Synechocystis*) [17] results in reaction rates comparable to the established heterotrophic production systems. Since then, a number of different enzyme classes were successfully employed in photobiotransformations. This review provides a short overview on methodological aspects of photobiotransformations and then focuses on the progress in the last few years on the increase of the productivity by metabolic engineering and alternative reaction systems for biotransformations. Other approaches such as production of biofuels from carbon dioxide (see reviews [95–97]) in metabolically engineered cyanobacteria expand the scope of this review and are not further discussed.

2 Methodology

Unicellular strains like *Synechocystis* and *Synechococcus elongatus* PCC 7942 (from now on *S. elongatus*) were intensively studied as host for biotransformations in wild-type cells [19–27] and recombinant cells [17, 28–37]. The ease of handling, well elucidated genetic background, simple morphology, and possible genetic modification made both strains model strains over the years. [38] Normalization and handling are complicated for filamentous strains like *Anabaena* sp. and *Nostoc* sp. and accurate cultivation procedures are required to ensure reproducibility. Examples of biotransformations in filamentous cyanobacteria are limited to wild-type cells [21, 39, 42]. Here, whole-cell biotransformations shall be defined by the targeted addition of a specific substrate that does not serve as carbon source. A common workflow often includes the following steps: (1) cyanobacteria are grown to a specific optical density, (2) cells are harvested and prepared for the biotransformation, and (3) the reaction is started by the addition of the substrate. The separation of cultivation and biotransformation allows the concentration of cells to increase space-time yields and the normalization to cell density, amount of chlorophyll *a* (chl*a*), or cell dry weight (CDW). Time samples of the reaction can be analyzed to monitor the reaction curve and to calculate specific activity and conversion.

Two strategies can be followed to genetically modify *Synechocystis* and *S. elongatus*: (1) genome integration via homologous recombination with subsequent segregation [17, 28–30, 33–36] and (2) self-replicative vectors [37]

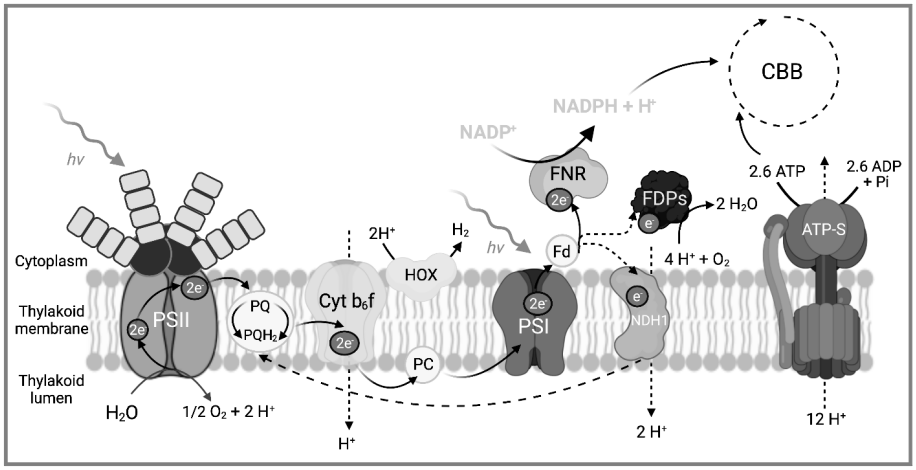

Figure 2. Overview of the photosynthetic electron transport chain in cyanobacteria. PSII, photosystem II; PQ, plastoquinone; PQH2, plastoquinol; Cyt *b6f*, cytochrome b_6f; PC, plastocyanin; HOX, NiFe hydrogenase; PSI, photosystem I; Fd, ferredoxin; FNR, ferredoxin NADP$^+$ reductase; FDPs, flavodiiron proteins; NDH1, NADH dehydrogenase complex 1; ATP-S, ATP synthase; CBB, Calvin-Benson-Bassham cycle. Adapted from Grimm et al. [18]. Created using biorender.com.

(Fig. 3). For the first strategy, an integrative vector is designed: the expression cassette is flanked by the regions that are homologous to the upstream and downstream sequence of the integration locus and includes the gene(s) of interest, important gene-regulating elements (GREs; e.g., ribosome binding site (RBS), promoter, terminator), and the resistance gene to exert selection pressure [43]. Genome integration generates stable mutant strains [44] but is time-expensive because of the segregation process, i.e., the integration of the expression cassette into every genome copy, which can take several weeks. The second strategy circumvents this by using self-replicative vectors that harbor the machinery for replication in several hosts [44]. However, copy number, stability, and constant antibiotic pressure need to be kept in mind and a higher variation between biological replicates can occur [45]. Examples are plasmids derived from pPMQAK1 [31, 32, 36, 46–48] and pSEVA [37, 49] with an RSF1010 origin. Recently, Opel et al. [45] expanded the available set of replicative plasmids by the pSOMA series. These chimeric plasmids are fusion constructs of the pSC101 replicon from *Escherichia coli* (*E. coli*) and the two smallest endogenous plasmids pCA2.4 and pCB2.4 from *Synechocystis* to enable both cloning in *E. coli* and maintenance in *Synechocystis* [45]. Production of GFP and the BVMO *Acidovorax* sp. CHX100 proved functional gene expression and the pSOMA plasmids were compatible with RSF1010-based plasmids, which increases flexibility in genetic modification [45]. Production of the same BVMO via genomic integration and using a pPMQAK1 derivative was compared by Tüllinghoff et al. and yielded 2.6-fold

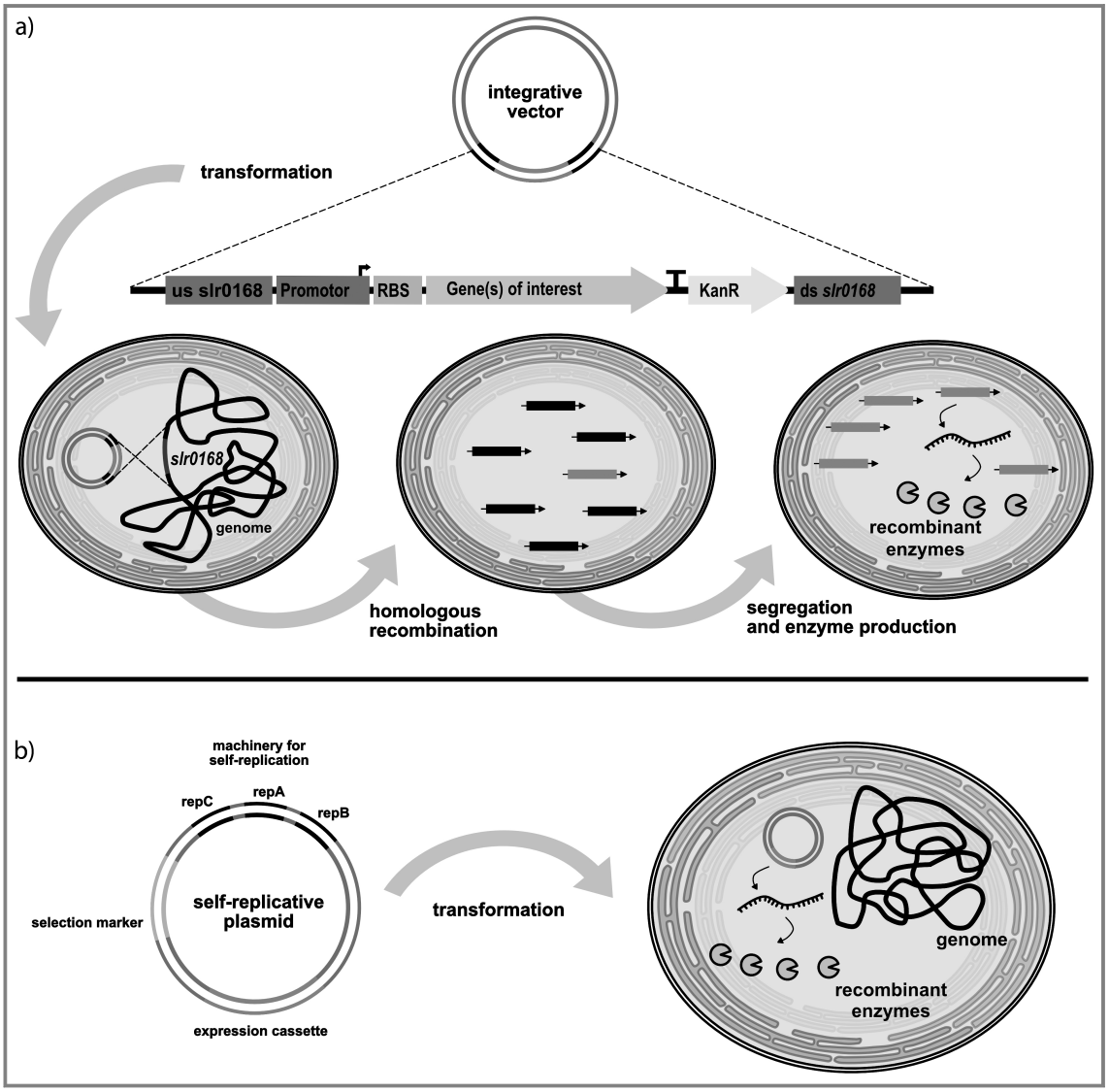

Figure 3. Strategies for the production of recombinant enzymes in cyanobacteria for light-driven biotransformations. a) The expression cassette is integrated into a neutral gene locus of the genome via homologous recombination. Integration into every genome copy (segregation) can take several weeks. b) Use of a plasmid that harbors the machinery for self-replication, e.g., based on RSF1010.

higher production with the plasmid-based expression system [36].

GREs allow some control over the amount of enzyme produced and are the "screws" for an adjustment of cell productivity. The review of Till et al. [50] provides a detailed overview of GREs for cyanobacteria. A major problem is the lack of inducible promoter systems that allow a flexible control of gene expression. Well-working promoter systems from other organisms like *E. coli* do not work as efficient in cyanobacteria [46, 51]. Lac-based promoters such as P_{trc} suffer from poor repression and inefficient induction [46, 51]. However, P_{trc} mediates strong constitutive gene expression in *Synechocystis* [46] and variants, e.g., P_{trc10} and $P_{trc.x.lacO}$, are often used for recombinant gene expression [31, 32, 37, 47, 48]. Commonly used native promoters are P_{rnpB} (promoter of ribonuclease P gene [46]), P_{rbcL} (promoter of the large subunit of Rubisco [46]), "super-strong" P_{cpc} (promoter of subunits for phycocyanin [52]), and light-inducible P_{psbA2} (promoter of D1 unit of PSII [53]), which all mediate moderate to strong gene expression and are constitutive (P_{psbA2} under illuminated cultivation conditions). The native promoters P_{zia} (promoter of P-type ATPase ZiaA [54]) and P_{nrsB} (promoter of the nrs operon involved in nickel tolerance [55]) are induced by Zn^{2+} and Co^{2+}/Ni^{2+}, respectively. Due to unspecific induction by several heavy metal ions [56, 57], its leakiness, and the generally weak strength [30, 43], P_{zia} is less suitable for biotechnological applications. In contrast, P_{nrsB} is tight and mediates moderate gene expression comparable to P_{psbA2} [58] and proved well for the expression of the BVMO from *Acidovorax* sp. CHX100 [36]. Risks of the use of metal-inducible promoters are the presence of metal ions in standard culture media and narrow induction range because metal ions become toxic in higher concentrations. [59, 60] Recently, rhaBAD promoter (P_{rha}) which is induced by L-rhamnose [59, 60] was described for application in *Synechocystis*. The promoter proved to be tight with a linear response and a good dynamic range upon L-rhamnose addition. L-Rhamnose is not metabolized and does not affect growth, which makes it an ideal inducer [59].

2.1 Native Cyanobacteria

Wild-type cyanobacteria were described for the light-driven reduction of aryl methyl ketones [19–24, 26, 27, 42, 61], terpenes [10, 16, 62–65], enones [64], hydrocortisone [66], and chalcones [40–42]. The reactions are catalyzed by enzymes of the natural pool inside the cell that are not further identified and remain unknown. This provides the chance to discover novel activities with potential biotechnological applications, like the conversion of xenobiotic oxophosphonates by *Nodularia sphaerocarpa* [39], and facilitates industrial process implementation because unmodified strains do not require gene safety regulations [67]. However, the low space time yields in combination with the small scope for optimization are the main drawbacks of biotransformations in wild-type cyanobacteria and a strong argument for genetically modified strains.

Beside cyanobacteria, other phototrophs were used for light-driven biotransformations [10, 11]. Böhmer et al. [11] first identified ene-reductases in the genome of unicellular microalgae *Chlamydomonas reinhardtii* (hereafter *C. reinhardtii*) and characterized the enzymes in vitro before whole-cell biotransformations were performed. This strategy allowed the identification of preferred substrates and the selectivity of the involved enzymes facilitating the setup of the whole-cell approach. Accordingly, the best substrate *N*-methylmaleimide was converted with a rate of 540 $\mu M\,h^{-1}$ by unmodified *C. reinhardtii* exceeding rates in wild-type cyanobacteria. [11] A completely different approach for the use of phototrophic organisms was presented by Löwe et al. [68]. The authors coupled light-driven reduction of CO_2 to formate in *C. reinhardtii* with the in situ catalyzed reaction of a formate dehydrogenase regenerating NADH to produce amines. Thus, *C. reinhardtii* is only used to recycle the electron mediator CO_2/formate but not as production host [68].

2.2 Recombinant Cyanobacteria

The current cyanobacterial photosynthetic activity, i.e., solar-to-biomass energy conversion, lies between 8 and 10 %. Major losses arise when the source, e.g., solar energy, exceeds the capacity of the sink metabolism. This could be alleviated by either dimming or dampening the light or through rewiring of the metabolism by heterologously expressing genes, which will serve as electron sinks [69, 70]. Tab. 1 lists the current light-driven biotransformations in recombinant cyanobacteria. Significant reaction parameters for cyanobacterial biotransformations such as light intensity, cell density as well as substrate concentration are included. Figs. 4 and 5 show examples for reductive biotransformation and oxyfunctionalization in recombinant cyanobacteria, respectively.

2.2.1 Reduction

Asymmetric reductions of C=C double bonds are relevant in biocatalysis to synthesize optically pure compounds. Fig. 4 shows various reduction reactions performed in recombinant cyanobacteria. Stereoselective alkene reduction is catalyzed by enoate reductases [EC 1.3.1.31] creating two chiral centers [71]. The gene of the ene-reductase YqjM from *Bacillus subtilis* (hereafter *B. subtilis*) was successfully integrated heterologously in the cyanobacterium *Synechocystis* under the control of P_{psbA2} and successfully converted various substrates delivering a maximum specific activity of 123 $U\,g_{CDW}^{-1}$ [17]. Moreover, optically pure product (> 99 % ee, (*R*)-2-methylsuccinimide) was obtained. This work provided a proof of concept that heterologous expres-

Table 1. Biotransformations in recombinant cyanobacteria. n.a., not available; n.c., not converted; CDW, cell dry weight; BVMO, Baeyer-Villiger monooxygenase; µE, $\mu mol_{photons} m^{-2} s^{-1}$; a, two-liquid phase system, 20 % (v/v) cyclohexane in diisononyl phthalate (DINP); b, reactions in a stirred-tank photobioreactor, 5 % (v/v) cyclohexane in DINP.

Organism	Reaction	Enzyme	Light intensity [µE]	Cell density [$g_{CDW} L^{-1}$]	Substrate	C_0 [mM]	Product	Conversion [%]	ee/de [%]	Specific activity [$U\ g_{CDW}^{-1}$]	Ref.
Synechocystis sp. PCC 6803	reduction of C=C bonds	ene-reductase from *B. subtilis*	150	0.36–2.70	cyclohexenone	15	cyclohexanone	70	n.a.	39	[17]
					2-methylcyclohexenone	15	2-methylcyclohexanone	42	n.a.	21.1	
					ketoisophorone	10	levodione	57	n.a.	6.2	
					cyclopentenone	15	cyclopentanone	99	n.a.	25.6	
					N-methylmaleimide	15	*N*-methylsuccinimide	94	n.a.	53.2	
					2-methylmaleimide	20	(*R*)-2-methylsuccinimide	99	> 99 (*R*)	90.9	
					2-methyl-*N*-methylmaleimide	20	2-methyl-*N*-methylsuccinimide	99	n.a.	99.5	
Synechocystis sp. PCC 6803	oxidation of various cyclic ketones	CHMO from *Acinetobacter* sp.	150	1.8	cyclohexanone	5	ε-caprolactone	n.a.	n.a.	2.3	[28]
					cyclohexen-2-one		cyclohexanone	n.c.	n.a.	n.c.	
					rac-2-methylcyclohexanone		7-methyloxepan-2-one	48	n.a.	2.0	
					rac-3-methylcyclohexanone		6-methyloxepan-2-one	72	n.a.	2.9	
					4-methylcyclohexanone		5-methyloxepan-2-one	82	n.a.	5.7	
					cyclopentanone		δ-valerolactone	> 99	n.a.	2.3	
					cyclopenten-2-one		cyclopentanone	n.c.	n.a.	n.c.	
					dihydrocarvone		7-methyl-4(prop-1-en-2-yl)oxepan-2-one	n.c.	n.a.	n.c.	

Continued Table 1.

Organism	Reaction	Enzyme	Light intensity [µE]	Cell density [$g_{CDW}L^{-1}$]	Substrate	C_0 [mM]	Product	Conversion [%]	ee/de [%]	Specific activity [$U\,g_{CDW}^{-1}$]	Ref.
Synechocystis sp. PCC 6803	reduction of cyclic imines	imine reductases (IRED-A) from *Streptomyces* sp. GF3587	150	3.6	2-methylpyrroline	8	2-methylpyrrolidine	84	> 94 (*R*)	21.8	[29]
					6-methyltetra-hydropyridine	4	2-methylpiperidine	61	> 94 (*R*)	8.9	
					7-methyltetrahydro-azepine	4	2-methylazepane	> 99	> 99 (*R*)	5.5	
					3,4-dihydroiso-quinoline	5	tetrahydroisoquinoline	99	n.a.	10.2	
					1-methyldihydro-isoquinoline	4	1-methyl-tetrahydro-isoquinoline	94	63 (*R*)	3.1	
					2,3,3-trimethylindole	5	2,3,3-trimethylindoline	26	94 (*R*)	1.6	
Synechocystis sp. PCC 6803	reduction of C=C bonds	ene-reductase from *B. subtilis*	150	2.4	2-methylmaleimide	10	(*R*)-2-methylsuccini-mide	> 99	n.a.	146.9	[30]
					N-methylmaleimide		*N*-methylsuccinimide	n.a.	n.a.	107.1	
					2-methyl-*N*-methyl-maleimide		2-methyl-*N*-methyl-succinimide	> 99	n.a.	132.7	
					cyclohexen-2-one		cyclohexanone	n.a.	n.a.	101.0	
					2-methylcyclo-hexenone			n.a.	n.a.	15.8	
Synechocystis sp. PCC 6803	terminal oxy-functionaliza-tion of nonanoic acid methyl ester	alkane mono-oxygenase AlkGBT from *Pseudomonas putida*	30	2.0	nonanoic acid methyl ester (NAME)	10	*ω*-hydroxynonanoic acid methyl ester	0.65	n.a.	0.9	[31]
Synechocystis sp. PCC 6803	terminal alkyl group oxyfunc-tionalization	alkane mono-oxygenase AlkGBT from *Pseudomonas putida*	30	1.9	nonanoic acid methyl ester	10	*ω*-hydroxynonanoic acid methyl ester	n.a.	n.a.	5.6	[47]
Synechocystis sp. PCC 6803	hydroxylation of cyclohexane	cytochrome P450 mono-oxygenase from *Acidovorax* sp. CHX100	150	0.5	cyclohexane	5	cyclohexanol	n.a.	n.a.	26.3	[32]
						a				39.2	
						b				34.9	

Continued Table 1.

Organism	Reaction	Enzyme	Light intensity [µE]	Cell density [$g_{CDW}L^{-1}$]	Substrate	C_0 [mM]	Product	Conversion [%]	ee/de [%]	Specific activity [$U\,g_{CDW}^{-1}$]	Ref.
Synechococcus elongatus PCC 7942	asymmetric conversion	*L. kefir* alcohol dehydrogenase	400	0.66	acetophenone	20 % (v/v)	(*R*)-1-phenylethanol	> 99	> 99 (*R*)	n.a.	[33]
Synechocystis sp. PCC 6803	oxyfunctionalization	BVMO from *Burkholderia xenovorans*	300	2.4	cyclohexanone	10	ε-caprolactone	> 99	n.a.	25	[35]
					rac-2-phenylcyclohexanone		(*R*)-7-phenyloxepan-2-one	> 99	> 99 (*R*)	n.a.	
Synechocystis sp. PCC 6803	oxyfunctionalization	BVMO from *Acidovorax* sp. CHX100	300	0.25–0.50	cyclohexanone	5	ε-caprolactone	n.a.	n.a.	60.9	[36]
Synechocystis sp. PCC 6803 Δ*hoxYH*	α-keto acid reduction	α-keto acid dehydrogenase from *Lactobacillus confusus* and *Lactobacillus paracasei*	215	2.24	phenyl pyruvic acid	10	2-hydroxy-3-phenylpropanoic acid	46	> 99 (*R*)	14.1	[37]
					4-methyl-2-oxovaleric acid		2-hydroxy-4-methylpentanoic acid	53	> 99 (*R*)	0.8	

sion of genes in cyanobacteria can exploit its photosynthetic machinery by providing and regenerating reducing cofactors such as NADPH or NADH. Furthermore, the atomic efficiency of the reaction is improved since no other co-substrates were utilized for cofactor regeneration. Chiral amines are valuable components of pharmaceutical compounds with an estimated 40–45 % of compounds containing chiral amine scaffolds. Several drawbacks of current chiral amine synthesis include the usage of toxic chemicals, by-product formation, and multistep syntheses [72]. Hence, biocatalytic methods to produce chiral amines are being explored and developed to address these limitations. In this regard, the genes of three imine reductases (IREDs) were expressed in *Synechocystis* and tested in the reduction of various imines [29]. By changing the promoter from P_{psbA2} to the strong P_{cpc} promoter, higher conversions were obtained in the reduction of 2-methylpyrroline. This indicated that the amount of enzyme was the limiting factor in the reaction. Toxicity effects of the substrates were also alleviated by increasing the cell density up to 6.0 $g_{CDW}L^{-1}$.

Alcohol dehydrogenases from *Lactobacillus kefir* (LkADH) produced in *S. elongatus* catalyzed the conversion of acetophenone to optically pure (*R*)-1-phenylethanol (ee > 99 %) [33]. Chiral phenylethanols are important precursors in the production of pharmaceuticals and fine chemicals. The LkADH gene was expressed under the control of the P_{psbA1} promoter and the effects of light and CO_2 concentration were evaluated. A doubling of the growth rate was observed upon cultivation at high light (400 µE) and elevated CO_2 concentration (1 %). Complete conversion of acetophenone was observed after 20 h using 0.66 g L^{-1} of cells under 0.5 % of CO_2. The addition of CO_2 during cultivation and during biotransformation was partially attributed to increased cyanobacterial growth. Furthermore, its addition also enhanced the availability and recyclability of NADPH.

Stereodiverse α-keto acids were reduced to their corresponding α-hydroxy acids using *Synechocystis* expressing the genes of α-keto acid dehydrogenases (KADH) [37]. KADHs, namely, L- and D-2-hydroxyisocaproate dehydrogenase from *Lactobacillus confusus* DSM 20196 (L-HicDH) and *Lactobacillus paracasei* DSM 20008 (D-HicDH), initially produced in *E. coli* displayed activities in the presence of both NADH and NADPH albeit reduced in the latter. Expression in cyanobacteria proved to be challenging and mutants containing both enzymes were only obtained in the Δ*hoxYH* background. This mutant is a markerless deletion mutant lacking the functional hydrogenase HOX as competing electron sink. Hence, comparison with the parent *Synechocystis* strain was not possible. Conversion of phenylpyruvic acid and 4-methyl-2-oxovaleric acid to their corresponding α-hydroxy acids reached 46 and 53 %, respectively, in high stereoselectivity (> 99 %) with the cyanobacterium expressing D-HicDH.

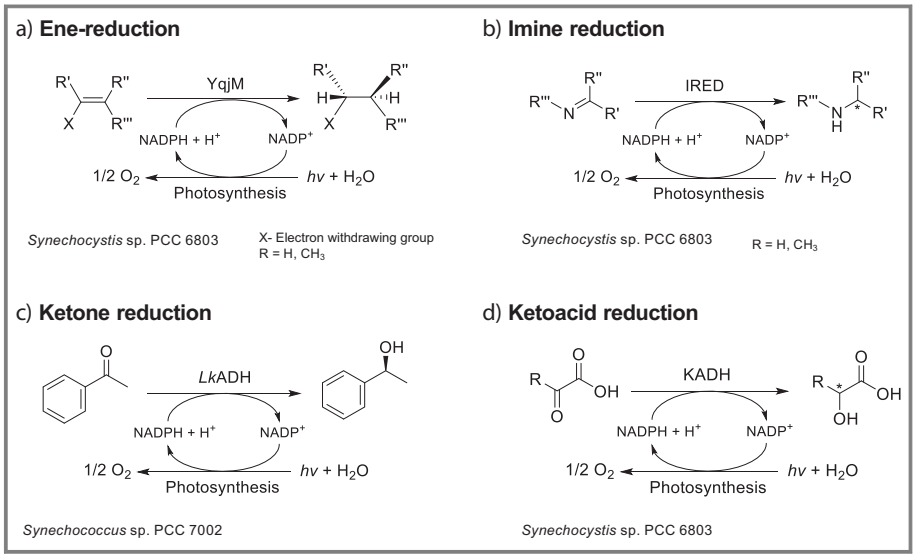

Figure 4. Examples of reduction reactions in recombinant cyanobacteria. Reducing equivalents in the form of NADPH are supplied and regenerated during photosynthesis while electrons are provided by water splitting from PSII. YqjM, ene-reductase from *B. subtilis*; IRED, imine reductases from *Streptomyces* sp. GF3587, *Kribbela flavida* DSM 17836, or *Saccharothrix espanaensis* ATCC 51144; LkADH, alcohol dehydrogenase from *Lactobacillus kefir*; KADH, α-keto acid dehydrogenases from *Lactobacillus confusus* or *Lactobacillus paracasei*.

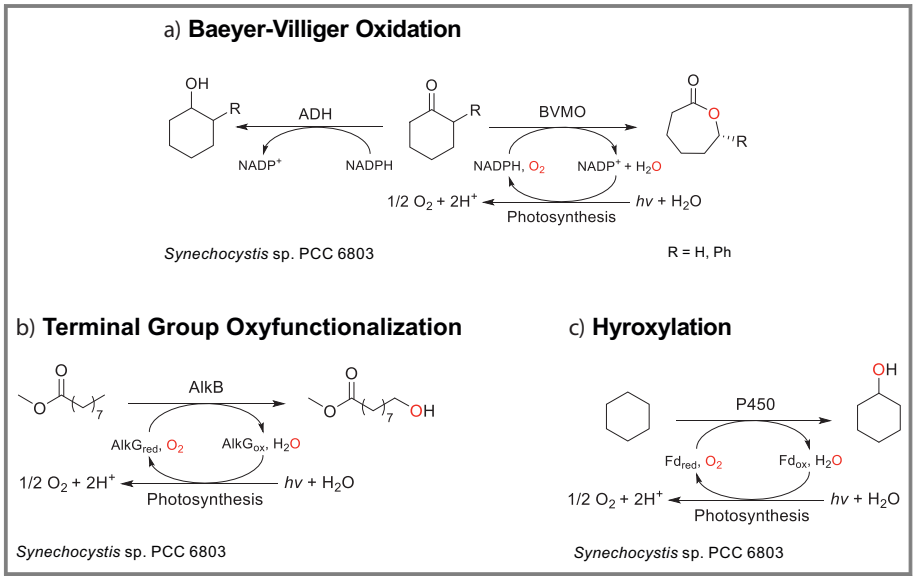

Figure 5. Examples of oxyfunctionalization reactions in recombinant cyanobacteria. Oxygen derived from photosynthetic water splitting is utilized as the oxidant for the reaction. In Baeyer-Villiger oxidation reactions, the ketone is reduced to its corresponding alcohol from the action of native alcohol dehydrogenases in cyanobacteria. ADH, alcohol dehydrogenases; BVMO, Baeyer-Villiger monooxygenases; AlkB, monooxygenase component from *Pseudomonas putida* GPo1; AlkG, rubredoxin; Fd, ferredoxin.

2.2.2 Oxyfunctionalization

Oxyfunctionalization reactions belong to the most important transformations in organic chemistry. Oxyfunctionalization involves integration of at least one oxygen atom into the product [18]. Conventionally, reactions involving oxygen require high reaction temperatures and/or pressures. This necessitates expensive process control regimes and generates safety issues [31]. Enzyme catalysis, on the other hand, could achieve high selectivities and yields while operating at milder conditions. Fig. 5 shows examples of oxyfunctionalization reactions in recombinant cyanobacteria. The gene of cyclohexanone monooxygenase (CHMO), perhaps the most widely-used Baeyer-Villiger monooxygenase (BVMO) from *Acinetobacter calcoaceticus* NCIMB 9871, was first cloned in *Synechocystis* to oxidize various cyclic ketones to their corresponding lactones [28]. The *chnB* gene was inserted into a cassette under the control of the light-inducible promoter P_{psbA2}. ε-Caprolactone, the product from the oxidation of cyclohexanone was detected after 24 h. However, the reaction did not go to completion due to the formation of a side-product, namely, cyclohexanol. This so-called ketoreduction was observed due to the presence of endogenous alcohol dehydrogenases in *Synechocystis*, which was also detected in the selective reduction of cinnamyl aldehyde [24, 39]. Specific activities ranging from 2–6 U g_{CDW}^{-1} were observed, which were comparable with rates achieved using the same enzyme in *E. coli* [73]. Ketoreduction, on the other hand, was also relatively high with a maximum of 50 % using cyclohexanone as the substrate. Interestingly, it was not observed when cyclopentanone was utilized albeit having similar specific activity as that of cyclohexanone. Product formation rates and, consequently, specific activities were lower as compared to that of the ene-reductase YqjM [17]. Nevertheless, this work has demonstrated that oxyfunctionalization reactions are feasible in cyanobacteria harboring oxidoreductases.

The newly discovered BVMO from *Burkholderia xenovorans* ($BVMO_{Xeno}$) showed higher activity in the whole-cell oxidation of cyclohexanone to ε-caprolactone both in *E. coli* and *Synechocystis* [35]. In *Synechocystis*, a ninefold higher specific activity was observed (18 vs 2 U g_{DCW}^{-1}) in $BVMO_{Xeno}$ as compared to $CHMO_{Acineto}$. [28] Interestingly, the catalyst turnover rate k_{cat} of $BVMO_{Xeno}$ is lower as compared to that of $CHMO_{Acineto}$, whereas K_M (substrate concentration to achieve $1/2V_{max}$) is higher, leading to a higher catalytic efficiency. Moreover, the thermostability and optimum pH of $BVMO_{Xeno}$ are slightly higher making it more favorable for application in *Synechocystis*. As the concentration of cyclohexanone inside of the cell is unknown, the exact reason for the higher activity in two different bacterial production systems remains unclear. Nevertheless, this is a striking example that enzymes can perform very differently in whole-cell biocatalysts and in cell-free systems. Recently, an NADPH-dependent BVMO gene from *Acidovorax* sp. CHX100 was heterologously expressed in *Synechocystis* to efficiently catalyze the oxyfunctionalization of cyclohexanone to ε-caprolactone [36]. The *Synechocystis* strain constructed using a Ni^{2+}-inducible P_{nrsB} promoter (*Syn*6803_Ni_pBVMO) showed a maximum specific activity of 52.2 U g_{CDW}^{-1}. Lower specific activities were observed when a Cu^{2+}-inducible system was utilized, which could be attributed to its slight leakiness. Specific activities increased concurrently with increased light intensities, reaching a maximum of 60.9 U g_{CDW}^{-1} (5.2 U mg_{chla}^{-1}). Residual activities were still observed even after the addition of PSII inhibitor 3-(3,4-dichlorophenyl)-1,1-dimethylurea or upon dark incubation, which are fueled by reducing equivalents derived from storage compounds as observed in reduction reactions [17]. *Syn*6803_Ni_pBVMO reached a product yield of 1.6 g g_{CDW}^{-1} in a 2-L photobioreactor, which is similar to an industrially-relevant BVMO-based process using *E. coli* (1.6 g g_{CDW}^{-1}) [74]. Initial and 24-h average productivity (187 mg $L^{-1}h^{-1}$ and 59 mg $L^{-1}h^{-1}$) are in the range of the highest productivities in cyanobacterial biotransformations.

The efficiency of photosynthesis-derived oxygen for catalyzing oxidation reactions was also demonstrated in the regioselective terminal oxyfunctionalization of nonanoic acid methyl ester (NAME) to 9-hydroxynonanic acid (H-NAME) [31, 47]. *Synechocystis* was genetically engineered to synthesize alkane monooxygenase AlkBGT from *Pseudomonas putida* GPo1 consisting of a rubredoxin reductase (AlkT), a rubredoxin (AlkG), and the monooxygenase component AlkB. Whole-cell biotransformations performed aerobically produced comparable oxidation rates with light and in the dark suggesting that catabolism of storage compounds from the latter condition is sufficient to regenerate NADPH. The specific production rate of 0.9 U g_{CDW}^{-1} corresponded to capturing nearly 25 % of photosynthetically-generated molecular O_2 [31]. The long-term applicability of the aforementioned *Synechocystis* harboring AlkBGT was demonstrated using a two-liquid phase system [32]. Compared to single aqueous phase biotransformations, a 1.7-fold increase in initial specific activity was observed when diisononyl phthalate (DINP) was utilized as an organic carrier solvent at an organic/aqueous ratio of 1:3. This was attributed to reduced cell toxification as well as substrate inhibition by decreased aqueous NAME concentrations. A high specific product yield of 3.8 mmol g_{CDW}^{-1} was observed when 50 % (v/v) of NAME in DINP was utilized. The system was then transferred to a 3-L photobioreactor equipped with an aeration system supplying compressed air, an altered light distribution, and an impeller for stirring. An increase of 36 % in initial specific activity was observed when 25 % (v/v) of NAME in DINP was utilized as compared to single aqueous phase systems. However, initial specific activity and specific yields were reduced by 54 and 50 %, respectively, when 50 % (v/v) was utilized indicating catalyst inactivation at high substrate concentrations.

2.3 Deleting Competing Pathways to Increase Productivity

Under fluctuating light intensities and nutrient availability, the CBB cycle becomes saturated resulting in excessive reduction of photosystem I (PSI). This results in the generation of reactive oxygen species (ROS) which could severely damage the photosynthetic machinery. Thus, cyanobacteria have developed photoprotection mechanisms and auxiliary transport systems to maintain PSI and its P700 reaction center chlorophyll in an oxidized state as well as to prevent photoinhibition [69, 75] (Fig. 6). Flavodiiron proteins (FDPs; Flv1–4) present in cyanobacteria reduce excess oxygen to water, which is commonly known as the Mehler-like reaction. FDPs, particularly Flv1 and Flv3, remove 60 % of excess electrons and convert them to water at high light conditions [76]. Moreover, the NADH dehydrogenase-like complex 1 (NDH1) existing in cyanobacteria participates in distinct cellular functions. It further oxidizes Fd and returns the electrons to the PQ pool. Furthermore, bidirectional hydrogenases encoded by the *hox* (hydrogen oxidation) genes constitute an electron sink [77]. Photoinhibition could also be alleviated by the cyanobacterial respiratory terminal oxidases such as cytochrome c oxidase (COX) and alternative respiratory terminal oxidase (ARTO) [78, 79].

The activity of cytochrome P450 (CYP1A1) produced in *Synechococcus* PCC 7002 was doubled when the subunit of the NDH1 was knocked out [80]. By expressing the P450 CYP1A1 gene in cyanobacteria, an ample supply of reducing equivalents are supplied and O_2 is photosynthetically generated. NdhD2, an NDH1 subunit, was removed to retain a functioning NDH1 complex. Using the EROD assay, a twofold increase of activity was shown by the deletion mutant as compared to its parent strain. Recently, CYP1A1 from *Rattus norvegicus* (Sy21) was expressed in *Synechococcus* sp. PCC 7002 with a deletion of the COX cluster (Sy21ΔCOX) [79]. A fourfold increase in activity

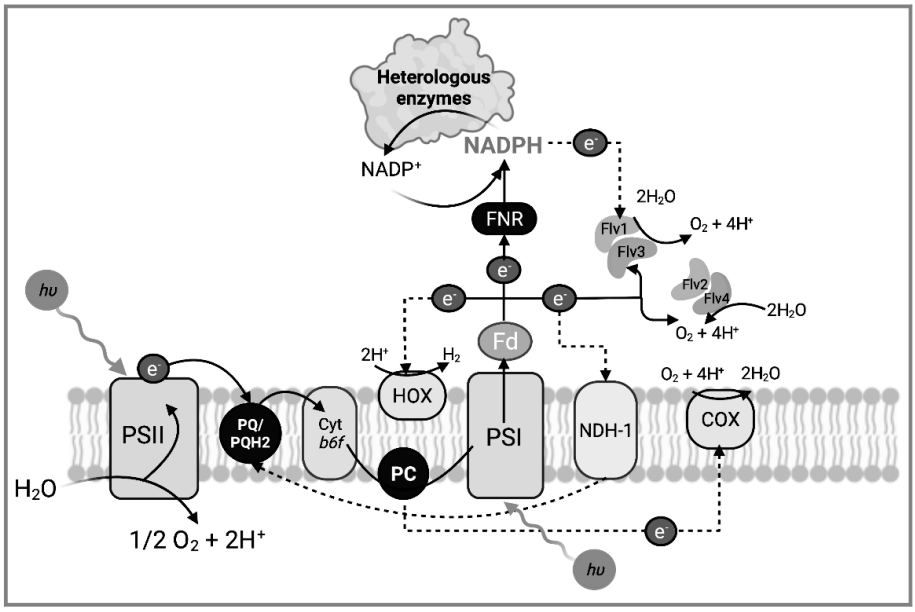

Figure 6. Simplified PETC showing possible electron sinks. Electrons from water are extracted in PSII upon illumination and are conveyed to plastocyanin, cytochrome b_6f, PSI, and, finally, to ferredoxin. The latter distributes the photosynthetic electrons to flavodiiron proteins, bidirectional hydrogenase (HOX), and to a subunit of type I NADH dehydrogenase (NDH1). Cyanobacterial respiratory terminal oxidases such as cytochrome c oxidase (COX) could also act as electron dissipation pathways. Created using biorender.com.

was observed when the deletion mutant was utilized as compared to the wild-type cyanobacterial strain. The presence of an additional electron sink increased the maximum electron transfer rate of PSII ($maxETR_{PSII}$) increasing the efficiency of photosynthesis. Moreover, a high $maxETR_{PSI}$ was observed in Sy21ΔCOX as compared to Sy21, indicating more electrons being transferred to PSI.

The deletion of flavodiiron proteins, i.e., Flv1 and Flv3, increased the activity of the ene-reductase YqjM expressed in *Synechocystis* [30]. A 2.5-fold increase in productivity was observed in the reduction of 2-methylmaleimide when the ΔFlv1 *Synechocystis* mutant producing YqjM (ΔFlv1::P_{cpc}YqjM) was utilized. Intracellular enzyme concentration remains unchanged suggesting that the increase in activity cannot be attributed to higher enzyme concentration but rather to funneling of electrons to the reaction. Recently, this concept was further demonstrated with two BVMOs from *Burkholderia xenovorans* ($BVMO_{Xeno}$) and *Parvibaculum lavamentivorans* ($BVMO_{Parvi}$) in the oxidation of cyclohexanone to ε-caprolactone [35]. By utilizing a ΔFlv1 knockout mutant, a 1.4 to 1.6-fold higher specific activity was obtained for both enzymes. While this shows the applicability of the activity increase by inactivation of electron-consuming enzymes for different enzyme classes, it is by no means conclusive evidence that the (highly regulated) photosynthetic electron transport chain was indeed successfully rerouted. To clarify this question, a comprehensive physiological analysis of the strains is necessary.

3 Influence of the Photobioreactor Geometry on the Productivity of Whole-Cell Biotransformations

For biotransformations to be economically feasible, a productivity of at least $1\,g\,L^{-1}h^{-1}$ is required to produce fine chemicals [81]. Despite having higher light capture capacity and further conversion into biomass as compared to higher plants, cyanobacteria still suffer from slow growth and low cell densities attributed to self-shading [82–84]. Hence, alternative reaction systems have been developed to address the efficient light uptake of cyanobacteria to fuel biotransformation reactions.

3.1 Immobilization on Films

Immobilizing photoautotrophs as films has already been performed specifically in the green algae *C. reinhardtii*, particularly for hydrogen production [85–87]. By immobilizing photosynthetic cells, the density increases, allowing improved light utilization on a per area basis [85]. Using this approach, "self-shading" on high cell density cultures could be circumvented. Moreover, by immobilizing cells, the light-to-product efficiency is improved due to uniform irradiation [88]. Fig. 7 shows the formation of cyanobacterial films employing high cell density (HCD) loadings. Vajravel et al. [89] demonstrated the application of a thin-layer biofilm technology to produce ethylene. The ethylene (C_2H_4)-forming enzyme (*efe*) from *Pseudomonas syringae* was produced in *Synechocystis*. Artificial biofilm was prepared using alginate, a natural polymer made up of guluronic and mannuronic acid residues. A formulation of 1 g wet cell biomass and 1 mL of 1 % alginate was utilized to prepare the film. A

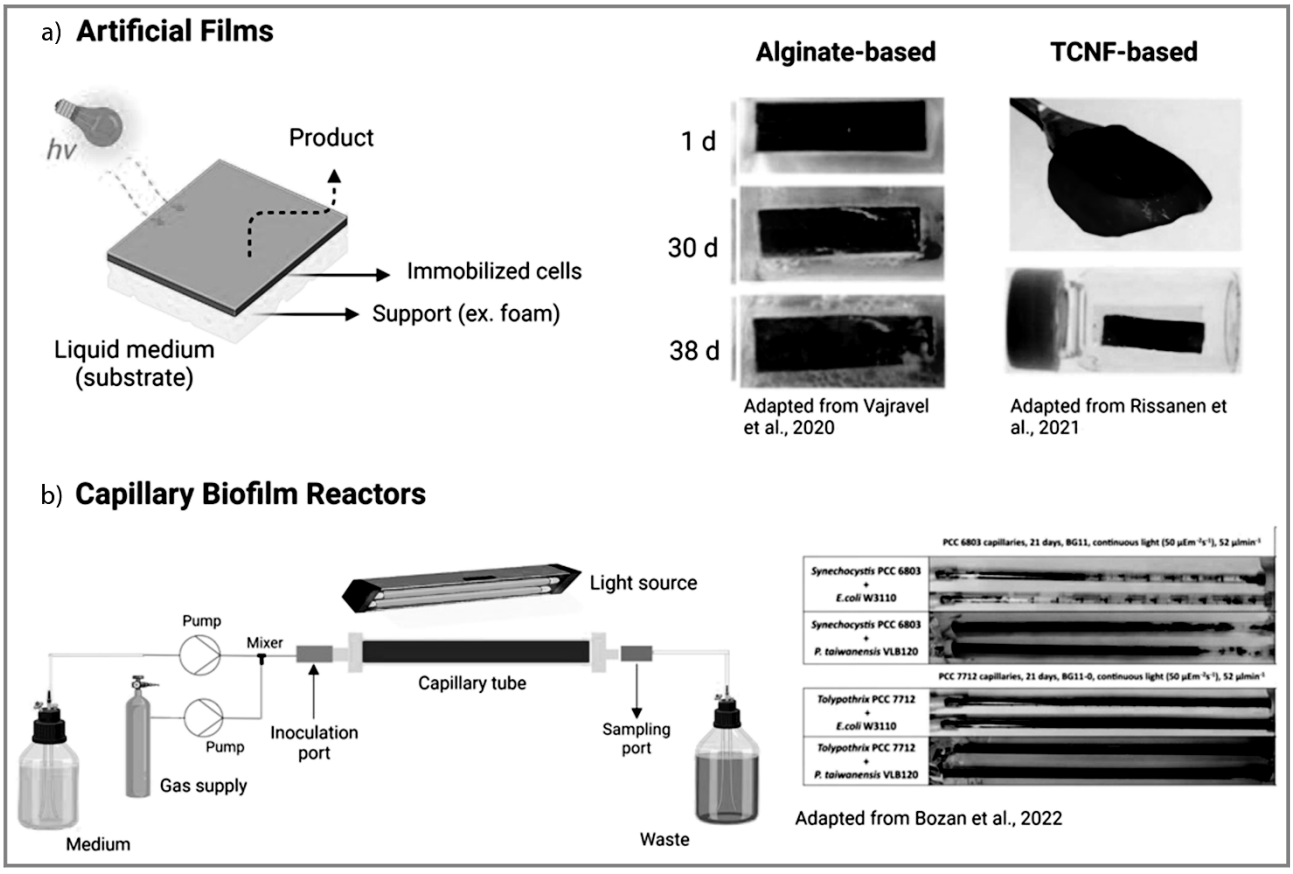

Figure 7. Immobilization of cyanobacteria as a) artificial biofilms and b) capillary biofilm reactors (CBRs). In artificial biofilms, a mixture of the cells and either sodium alginate or TCNF are combined followed by spraying with a solution of $CaCl_2$ to initiate polymerization. CBRs have a diameter of 3 mm. A peristaltic pump operating at 52 μL min^{-1} was utilized to deliver media and air to the system. An LED light system delivering a light intensity of 50–60 μE was installed on top of the capillary tube. Reaction setup adapted from Bozan et al. [90] Created using biorender.com.

water-insoluble matrix was achieved by spraying with a calcium chloride ($CaCl_2$; 50 mM) solution. The films were placed on top of a foam sponge as support. Initial studies using suspension systems showed optimal product formation using a bicarbonate (HCO_3^-) concentration of 200 mM as an inorganic carbon source and a moderate light intensity (35 μE). These parameters were then adapted for reactions using Ca^{2+}-alginate films. *Synechocystis efe* cells immobilized in films performed better than suspension systems sustaining ethylene production for 7 cycles (38 d) corresponding to ca 383 $mmol_{C2H4}mg_{chla}^{-1}$. Furthermore, a higher light-to-ethylene conversion was observed on films (0.35 %) as compared to suspension systems (0.10 %). These results revealed that thin-layer immobilization of cyanobacteria could improve the productivity by limiting biomass accumulation, thereby, focusing on the reaction at hand as well as maintaining cell fitness for prolonged periods.

The concept of photosynthetic cell factories (PCFs) was further demonstrated with the same *Synechocystis* strain harboring *efe*. The cells were entrapped within never-dried hydrogel films of 2,2,6,6-tetramethylpiperidine-1-oxyl (TEMPO)-oxidized cellulose nanofibers (TCNF) cross-linked with polyvinyl alcohol (PVA) creating self-standing architectures [88]. These self-standing matrix architectures were derived from never-dried native celluloses, e.g., bleached sulfite wood pulp, cotton, tunicin, and bacterial cellulose, which were disintegrated into their individual microfibrils after oxidation by TEMPO radical [91]. The nanocellulose-based matrix displays superior mechanical stability in terms of wet strength as compared to conventionally utilized alginate systems [89]. Using 200 mM of $NaHCO_3$ as an inorganic carbon source for C_2H_4 production in a submerged system, Ca^{2+}-alginate-based films disintegrated, releasing the cells into the medium. This was caused by the disruption of bonds between alginate and Ca^{2+} due to the formation of $CaCO_3$ upon $NaHCO_3$ addition. On the other hand, PVA-Ca^{2+}-TCNF-based films remained stable during the course of the reaction (8 d). An increase of 38 % in C_2H_4 production was observed using PVA-Ca^{2+}-TCNF-based films as compared to Ca^{2+}-alginate-based films.

Another approach to increase the cell density of cyanobacteria in biotransformation reactions is through utilization of capillary reactors. The remarkably high surface

area/volume ratio of capillary reactors enables low light penetration, thereby, increasing light to chemical energy conversion [92]. CBRs have an exceptionally high surface area/volume ratio of 1333–4000 m^2m^{-3} and low light penetration permitting higher cell loading without light limitation. A dual-species HCD was demonstrated consisting of the O_2-evolving *Synechocystis* and O_2-respiring *Pseudomonas taiwanensis* VLB120 for the continuous cyclohexane oxyfunctionalization [48]. Both species were heterologously expressed with cyclohexane monooxygenase using pAH050. A biofilm with a dry weight of 48 $g_{BDW}L^{-1}$ corresponding to 85 % of cyanobacteria was produced. A volumetric productivity of 0.2 $g\,L^{-1}h^{-1}$ was recorded over a one-month period. This biological system reached 98.9 % cyclohexane conversion and an 84.5 % reaction selectivity towards cyclohexanol. Recently, Bozan et al. [90] evaluated several cyanobacterial films for application in a novel capillary biofilm reactor. Several advantages of biofilm include: 1) resilience to external environments, 2) infinite turnover number, and 3) higher biomass loading (up to 60 $g_{CDW}L^{-1}$) as compared to suspended cell cultures (4–8 $g_{CDW}L^{-1}$). The CBR was composed of a capillary tube made of polymethylmethacrylate (PMMA; *ID* = 3 mm), a peristaltic pump delivering a flow rate of 52 $\mu L\,min^{-1}$, and an LED light system delivering a light intensity of 50–60 $\mu mol\,m^{-2}s^{-1}$ (Fig. 6b). Unicellular growing cyanobacteria, such as *Synechocystis* sp., *Synechococcus* sp., and *Cyanothece* sp., were compared to filamentous types, i.e., *Tolypothrix* sp., *Nostoc* sp., and *Leptolyngbya* sp., for their ability to form biofilms. *Tolypothrix* PCC 7712 was found to be the best candidate for film formation in combination with *P. taiwanensis* showing a threefold higher biomass production (62.6 $g_{BDW}L^{-1}$ and 2000 $mg_{chla}L^{-1}$) as compared to *Synechocystis*. Hydrogen production was constant over 14 d, reaching a concentration of 1.23 $mmol\,L^{-1}$ and a production rate of 0.14 $\mu mol_{H2}mg_{chla}{}^{-1}h^{-1}$.

3.2 Internally Illuminated Photobioreactors

Scalability of photobioreactors is still limited due to an additional parameter: light. In photobioreactor (PBR) design, light transmittance decreases exponentially with the distance from the source [93]. Due to these constraints, photobiotransformations are usually employed at small scale ($V \leq 10$ mL) and at low cell densities (< 10 $g_{CDW}L^{-1}$). The latter requirement is due to "self-shading" where cells obscure each other resulting in non-homogeneous light distribution [18]. Other important factors to consider are photoinhibition, CO_2 dispersion as well as O_2 degassing [84]. Current PBR systems are 1) membrane PBR, 2) bubble column PBR, 3) hybrid PBR, 4) airlift PBR, 5) tubular PBR, and 6) biofilm PBR [83].

To alleviate self-shading caused by external light sources, Hobisch et al. [34] performed ene-reduction in an internally illuminated bubble column PBR using *Synechocystis* harboring YqjM. The PBR consists of a glass cylinder (*ID* = 5 cm, *h* = 50 cm) fitted with emitting coils having a working volume of 0.2–0.8 L. Aeration was supplied at 0.6 $mL\,min^{-1}$ using an air pump sparged at the bottom of the reactor. Illumination was provided by wireless light emitters (WLEs) consisting of a white LED and a receiving coil enclosed in a polycarbonate shell (Fig. 8). This reactor concept was initially developed by Heining et al. [94] for the cultivation of *C. reinhardtii*. The presence of an intermediate frequency electromagnetic field (IF-EMF) as well as floating WLEs did

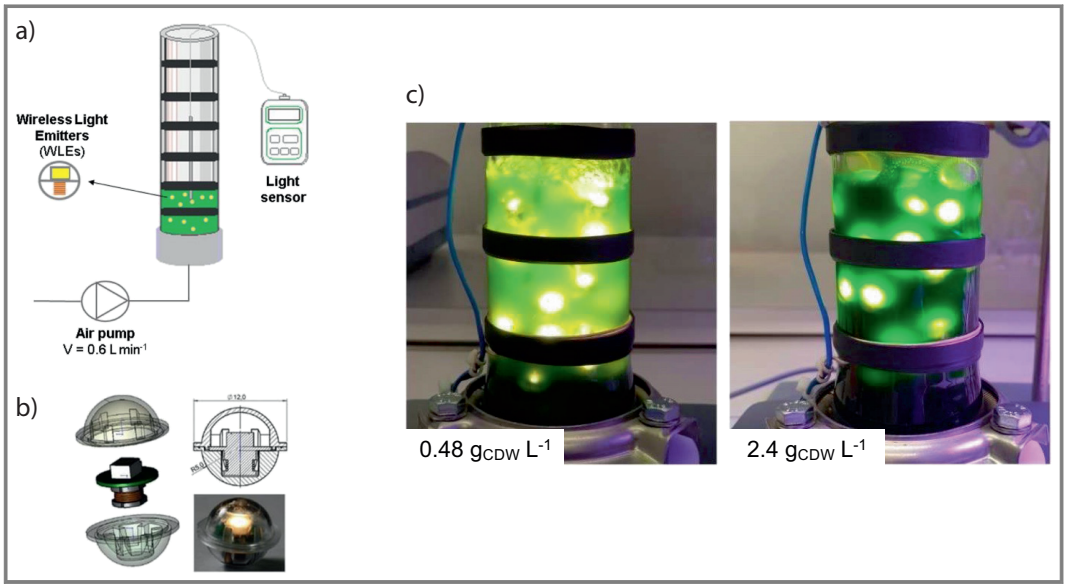

Figure 8. Bubble column reactor utilized for the reduction of 2-methylmaleimide in *Synechocystis* harboring the ene-reductase YqjM from *B. subtilis*. a) Reaction setup, b) wireless light emitters, and c) actual set showing different cell densities at a working volume of 200 mL. Adapted from Hobisch et al. [34].

not have a negative effect on the cells' growth rate and maximum photosynthetic yield. This WLE concept was also utilized in the decarboxylation of hexadecanoic acid (palmitic acid) into pentadecane [7]. Heterologously expressed *Cv*FAP (fatty acid decarboxylase from *Chlorella variabilis* NC64A) in *E. coli* catalyzed the formation of pentadecane from palmitic acid. Using 40 WLEs, complete conversion was achieved after 20 min as compared to 90 % conversion after 8 h for externally illuminated reaction system. The 22-fold increase in product formation was due to a higher light intensity provided by WLEs. Comparing product formation rates at similar light intensity showed a 1.8-fold increase in initial product formation rates highlighting the advantage of internally illuminated BCRs [7]. By using 40 WLEs and 2.4 $g_{CDW}L^{-1}$ of cells, full conversion of 2-methylmaleimide was obtained after 3.5 h with a specific activity of 32.5 U g_{CDW}^{-1} and a product formation of 3.7 mM h^{-1} [34]. A twofold rate increase was observed as compared to external illumination provided by LED strips demonstrating the clear advantage of internal illumination by WLEs. Furthermore, enantiopure (*R*)-2-methylsuccinimide at 73 % yield was obtained from 40 mM of 2-methylmaleimide. Purification of the product was not necessary, highlighting the practical application of cyanobacterial biotransformation.

4 Conclusions and Perspectives

Cyanobacteria have emerged as efficient production systems for light-driven redox reactions due to their capability to produce reducing equivalents, i.e., NADPH, and molecular oxygen fueling various reactions. The genetic toolbox is constantly being expanded to overcome the lack of a well-controlled inducible promoter system and to expand the available vector systems. Recombinant genes of oxidoreductases can be expressed either through genome integration or using self-replicative vectors, which increases the photon-to-product conversion efficiency. Furthermore, the potential of rational engineering of the photosynthetic electron transport chain remains largely untapped. One of the major limitations in scaling-up of cyanobacterial biotransformations is the provision of light. Alternative reaction systems to address this limitation are film formation and the utilization of internal illumination. Further work is needed to translate these approaches into industrially-feasible production systems. Continuous flow processes could be a potential route for upscaling and optimization since light penetration is uniform regardless of the reactor scale.

This project has received funding from the FET Open grant agreement 899576 (FuturoLEAF) (European Commission).

Lenny Malihan-Yap studied Chemical Engineering (B.Sc.) at the University of the Philippines Los Baños, Philippines. In 2016, she earned her doctorate degree (combined Masters and Ph.D.) in Energy Science and Technology from Myongji University, South Korea working on catalyst synthesis based on ionic liquids for biofuel applications. Currently, she is a postdoctoral researcher at the Institute of Molecular Biotechnology at Graz University of Technology, Graz, Austria. Her research interest includes biocatalysis using cyanobacteria harboring oxidoreductases, catalyst immobilization, and reactor design for biotransformation scale-up.

Hanna C. Grimm is a Ph.D. student at Graz University, Institute of Molecular Biotechnology under the supervision of Prof. Kourist. She studied Biochemistry with focus on biotechnology at University of Greifswald, Germany. During bachelor studies in 2014, she obtained the DAAD scholarship "RISE worldwide" for a summer research stay at the laboratory of Prof. Heinemann in London, ON, Canada. In 2017, she finished her master thesis under supervision of Prof. Bornscheuer in the field of biocatalysis. In Graz, she now specializes in light-driven whole-cell biotransformations in recombinant cyanobacteria. Her research interests include molecular biotechnology and enzyme engineering.

Robert Kourist is a full Professor and Head of the Institute of Molecular Biotechnology at Graz University of Technology, Graz, Austria and leader of the area Biotransformation at the Austrian Center of Industrial Biotechnology. He received his diploma and doctorate degree in Biochemistry from the University of Greifswald, Germany in 2006 under the supervision of Prof. Bornscheuer. He was a postdoctoral fellow in 2008 at the laboratory of Prof. Miyamoto at the Keio University in Yokohama, Japan. In 2009, he received the DSM Science and Technology Award North and a 1st prize in the VentureCup Mecklenburg-Vorpommern. In 2015, he was appointed member of the Young College of the Academy of Sciences and Arts of North Rhine-Westphalia. From 2012 to 2016, he was Junior Professor for Microbial Biotechnology at Ruhr-University Bochum. Dr. Kourist's expertise lies in the field of biocatalysis with a special focus on the development of chemo-enzymatic cascade reactions and light-catalyzed redox reactions. He has co-authored more than 100 publications and patents (H-index = 27).

Symbols used

C_0	[mM]	initial substrate concentration
ID	[mm]	internal diameter
k_{cat}	[s^{-1}]	catalyst turnover rate
K_M	[mM]	substrate concentration to achieve $1/2 V_{max}$
V_{max}	[mM s^{-1}]	maximal velocity of the reaction

Abbreviations

AlkB	monooxygenase component from *Pseudomonas putida*
AlkG	rubredoxin
AlkT	rubredoxin reductase
ARTO	alternative respiratory terminal oxidase
ATP	adenosine triphosphate
ATP-S	ATP synthase
B. subtilis	*Bacillus subtilis*
BVMO	Baeyer-Villiger monooxygenase
C. reinhardtii	*Chlamydomonas reinhardtii*
CBB	Calvin-Benson-Bassam
CBR	capillary biofilm reactor
CDW	cell dry weight
chl*a*	chlorophyll *a*
CHMO	cyclohexanone monooxygenase
COX	cytochrome c oxidase
*Cv*FAP	fatty acid decarboxylase from *Chlorella variabilis* NC64A
CYP1A1	cytochrome P450 from *Rattus norvegicus*
Cyt *b6f*	cytochrome b_6f
D-HicDH	L-2-hydroxyisocaproate dehydrogenase from *Lactobacillus paracasei*
DINP	diisononyl phthalate
E. coli	*Escherichia coli*
EPCS	enzyme-photocatalyst-coupled systems
FAP	fatty acid photodecarboxylase
Fd	ferredoxin
FDP	flavodiiron protein
FNR	ferredoxin $NADP^+$ reductase
GRE	gene-regulating elements
HCD	high cell density
H-NAME	9-hydroxynonanoic acid
hox	hydrogen oxidation
HOX	NiFe hydrogenase
IF-EMF	intermediate frequency electromagnetic field
IRED	imine reductase
KADH	α-keto acid dehydrogenase from *Lactobacillus confusus* or *Lactobacillus paracasei*
L-HicDH	L-2-hydroxyisocaproate dehydrogenase from *Lactobacillus confusus*
LkADH	alcohol dehydrogenase from *Lactobacillus kefir*
LPOR	light-dependent protochlorophyllide reductase
NADPH	reduced nicotinamide adenine dinucleotide phosphate
NAME	nonanoic acid methyl ester
NDH1	NADH dehydrogenase complex 1
PBR	photobioreactor
PC	plastocyanin
PCF	photosynthetic cell factories
PMMA	polymethylmethacrylate
PQ	plastoquinone
PQH2	plastoquinol
PSI	photosystem I
PSII	photosystem II
PVA	polyvinyl alcohol
RBS	ribosome binding site
ROS	reactive oxygen species
S. elongatus	*Synechococcus elongatus* PCC 7942
Synechocystis	*Synechocystis* sp. PCC 6803
TCNF	TEMPO-oxidized cellulose nanofibers
TEMPO	2,2,6,6-tetramethylpiperidine-1-oxyl
WLE	wireless light emitters

References

[1] C. J. Seel, T. Gulder, *ChemBioChem* **2019**, *20*, 1871–1897. DOI: https://doi.org/10.1002/cbic.201800806

[2] L. Schmermund, V. Jurkaš, F. F. Özgen, G. D. Barone, H. C. Büchsenschütz, C. K. Winkler, S. Schmidt, R. Kourist, W. Kroutil, *ACS Catal.* **2019**, *9*, 4115–4144. DOI: https://doi.org/10.1021/acscatal.9b00656

[3] U. M. Dikbas, M. Tardu, A. Canturk, S. Gul, G. Ozcelik, I. Baris, N. Ozturk, I. H. Kavakli, *Biochemistry* **2019**, *58*, 4352–4360. DOI: https://doi.org/10.1021/acs.biochem.9b00766

[4] L. Schmermund, S. Bierbaumer, V. K. Schein, C. K. Winkler, S. Kara, W. Kroutil, *ChemCatChem* **2020**, *12*, 4044–4051. DOI: https://doi.org/10.1002/cctc.202000561

[5] Y. Sun, E. Calderini, R. Kourist, *ChemBioChem* **2021**, *22*, 1833–1840. DOI: https://doi.org/10.1002/cbic.202000851

[6] W. Xu, Y. Chen, D. Li, Z. Wang, J. Xu, Q. Wu, *Mol. Catal.* **2022**, *524*, 112261. DOI: https://doi.org/10.1016/j.mcat.2022.112261

[7] H. T. Duong, Y. Wu, A. Sutor, B. O. Burek, F. Hollmann, J. Z. Bloh, *ChemSusChem* **2021**, *14*, 1053–1056. DOI: https://doi.org/10.1002/cssc.202002957

[8] F. F. Özgen, M. E. Runda, S. Schmidt, *ChemBioChem* **2021**, *22*, 790–806. DOI: https://doi.org/10.1002/cbic.202000587

[9] L. O. Björn, *Photochem. Photobiol.* **2018**, *94*, 459–465. DOI: https://doi.org/10.1111/php.12892

[10] L. Balcerzak, J. Lipok, D. Strub, S. Lochyński, *J. Appl. Microbiol.* **2014**, *117*, 1523–1536. DOI: https://doi.org/10.1111/jam.12632

[11] S. Böhmer, C. Marx, Á. Gómez-Baraibar, M. M. Nowaczyk, D. Tischler, A. Hemschemeier, T. Happe, *Algal Res.* **2020**, *50*, 101970. DOI: https://doi.org/10.1016/j.algal.2020.101970

[12] D. Kannchen, J. Zabret, R. Oworah-Nkruma, N. Dyczmons-Nowaczyk, K. Wiegand, P. Löbbert, A. Frank, M. M. Nowaczyk, S. Rexroth, M. Rögner, *Biochim. Biophys. Acta, Bioenerg.* **2020**, *1861*, 148208. DOI: https://doi.org/10.1016/j.bbabio.2020.148208

[13] A. Melis, *Plant Sci.* **2009**, *177*, 272–280. DOI: https://doi.org/10.1016/j.plantsci.2009.06.005

[14] N. E. Nozzi, J. W. K. Oliver, S. Atsumi, *Front. Bioeng. Biotechnol.* **2013**, *1*, 7. DOI: https://doi.org/10.3389/fbioe.2013.00007

[15] C. J. Knoot, J. Ungerer, P. P. Wangikar, H. B. Pakrasi, *J. Biol. Chem.* **2018**, *293*, 5044–5052. DOI: https://doi.org/10.1074/jbc.R117.815886

[16] F. Jüttner, R. Hans, *Appl. Microbiol. Biotechnol.* **1986**, *25*, 52–54. DOI: https://doi.org/10.1007/BF00252512

[17] K. Köninger, Á. Gómez Baraibar, C. Mügge, C. E. Paul, F. Hollmann, M. M. Nowaczyk, R. Kourist, *Angew. Chem., Int. Ed.* **2016**, *55*, 5582–5585. DOI: https://doi.org/10.1002/anie.201601200

[18] H. C. Grimm, E. Erdem, R. Kourist, in *The Autotrophic Biorefinery* (Eds: R. Kourist, S. Schmidt), De Gruyter, Berlin **2021**.

[19] K. Nakamura, R. Yamanaka, K. Tohi, H. Hamada, *Tetrahedron Lett.* **2000**, *41*, 6799–6802. DOI: https://doi.org/10.1016/S0040-4039(00)01132-1

[20] K. Nakamura, R. Yamanaka, *Chem. Commun.* **2002**, *2*, 1782–1783. DOI: https://doi.org/10.1039/b203844g

[21] J. Havel, D. Weuster-Botz, *Eng. Life Sci.* **2006**, *6*, 175–179. DOI: https://doi.org/10.1002/elsc.200620909

[22] T. Takemura, K. Akiyama, N. Umeno, Y. Tamai, H. Ohta, K. Nakamura, *J. Mol. Catal. B: Enzym.* **2009**, *60*, 93–95. DOI: https://doi.org/10.1016/j.molcatb.2009.03.017

[23] R. Yamanaka, K. Nakamura, A. Murakami, *AMB Express* **2011**, *1*, 24. DOI: https://doi.org/10.1186/2191-0855-1-24

[24] R. Yamanaka, K. Nakamura, M. Murakami, A. Murakami, *Tetrahedron Lett.* **2015**, *56*, 1089–1091. DOI: https://doi.org/10.1016/j.tetlet.2015.01.092

[25] S. Tanaka, H. Kojima, S. Takeda, R. Yamanaka, T. Takemura, *Tetrahedron Lett.* **2020**, *61*, 151973. DOI: https://doi.org/10.1016/j.tetlet.2020.151973

[26] J. Fan, Y. Zhang, P. Wu, X. Zhang, Y. Bai, *Bioorg. Chem.* **2022**, *118*, 105477. DOI: https://doi.org/10.1016/j.bioorg.2021.105477

[27] K. I. Itoh, K. Nakamura, T. Aoyama, T. Kakimoto, M. Murakami, T. Takido, *Tetrahedron Lett.* **2014**, *55*, 435–437. DOI: https://doi.org/10.1016/j.tetlet.2013.11.049

[28] S. Böhmer, K. Köninger, Á. Gómez-Baraibar, S. Bojarra, C. Mügge, S. Schmidt, M. M. Nowaczyk, R. Kourist, *Catalysts* **2017**, *7*, 240. DOI: https://doi.org/10.3390/catal7080240

[29] H. Büchsenschütz, V. Vidimce-Risteski, B. Eggbauer, S. Schmidt, C. Winkler, J. H. Schrittwieser, W. Kroutil, R. Kourist, *ChemCatChem* **2020**, *12*, 726–730. DOI: https://doi.org/10.1002/cctc.201901592

[30] L. Assil-Companioni, H. C. Büchsenschütz, D. Solymosi, N. G. Dyczmons-Nowaczyk, K. K. F. Bauer, S. Wallner, P. MacHeroux, Y. Allahverdiyeva, M. M. Nowaczyk, R. Kourist, *ACS Catal.* **2020**, *10*, 11864–11877. DOI: https://doi.org/10.1021/acscatal.0c02601

[31] A. Hoschek, B. Bühler, A. Schmid, *Angew. Chem., Int. Ed.* **2017**, *56*, 15146–15149. DOI: https://doi.org/10.1002/anie.201706886

[32] A. Hoschek, B. Bühler, A. Schmid, *Biotechnol. Bioeng.* **2019**, *116*, 1887–1900. DOI: https://doi.org/10.1002/bit.27006

[33] A. Sengupta, A. V. Sunder, S. V. Sohoni, P. P. Wangikar, *J. Biotechnol.* **2019**, *289*, 1–6. DOI: https://doi.org/10.1016/j.jbiotec.2018.11.002

[34] M. Hobisch, J. Spasic, L. Malihan-Yap, G. D. Barone, K. Castiglione, P. Tamagnini, S. Kara, R. Kourist, *ChemSusChem* **2021**, *14*, 3219–3225. DOI: https://doi.org/10.1002/CSSC.202100832

[35] E. Erdem, L. Malihan-Yap, L. Assil-Companioni, H. Grimm, G. D. Barone, C. Serveau-Avesque, A. Amouric, K. Duquesne, V. De Berardinis, Y. Allahverdiyeva, V. Alphand, R. Kourist, *ACS Catal.* **2022**, *12*, 66–72. DOI: https://doi.org/10.1021/acscatal.1c04555

[36] A. Tüllinghoff, M. B. Uhl, F. E. H. Nintzel, A. Schmid, B. Bühler, J. Toepel, *Front. Catal.* **2022**, *1*, 780474. DOI: https://doi.org/10.3389/fctls.2021.780474

[37] V. Jurkaš, C. K. Winkler, S. Poschenrieder, P. Oliveira, C. C. Pacheco, E. A. Ferreira, F. Weissensteiner, P. De Santis, S. Kara, R. Kourist, P. Tamagnini, W. Kroutil, *Eng. Microbiol.* **2022**, *2*, 100008. DOI: https://doi.org/10.1016/j.engmic.2021.100008

[38] C. Cassier-Chauvat, V. Blanc-Garin, F. Chauvat, *Genes* **2021**, *12*, 500. DOI: https://doi.org/10.3390/genes12040500

[39] M. Górak, E. Zymańczyk-Duda, *Green Chem.* **2015**, *17*, 4570–4578. DOI: https://doi.org/10.1039/c5gc01195g

[40] B. Zyszka, M. Aniol, J. Lipok, *Microb. Cell Fact.* **2017**, *16*, 136. DOI: https://doi.org/10.1186/s12934-017-0752-3

[41] B. Żyszka-Haberecht, A. Poliwoda, J. Lipok, *Appl. Microbiol. Biotechnol.* **2018**, *102*, 7097–7111. DOI: https://doi.org/10.1007/s00253-018-9109-z

[42] B. Żyszka-Haberecht, A. Poliwoda, J. Lipok, *J. Biotechnol.* **2019**, *293*, 36–46. DOI: https://doi.org/10.1016/j.jbiotec.2019.01.005

[43] E. Englund, J. Andersen-Ranberg, R. Miao, B. Hamberger, P. Lindberg, *ACS Synth. Biol.* **2015**, *4*, 1270–1278. DOI: https://doi.org/10.1021/acssynbio.5b00070

[44] L. Al-Haj, Y. Lui, R. Abed, M. Gomaa, S. Purton, *Life* **2016**, *6*, 42. DOI: https://doi.org/10.3390/life6040042

[45] F. Opel, N. A. Siebert, S. Klatt, A. Tüllinghoff, J. G. Hantke, J. Toepel, B. Bühler, D. J. Nürnberg, S. Klähn, *ACS Synth. Biol.* **2022**, *11*, 1758–1771. DOI: https://doi.org/10.1021/acssynbio.1c00605

[46] H. H. Huang, D. Camsund, P. Lindblad, T. Heidorn, *Nucleic Acids Res.* **2010**, *38*, 2577–2593. DOI: https://doi.org/10.1093/nar/gkq164

[47] A. Hoschek, J. Toepel, A. Hochkeppel, R. Karande, B. Bühler, A. Schmid, *Biotechnol. J.* **2019**, *14*, 1800724. DOI: https://doi.org/10.1002/biot.201800724

[48] A. Hoschek, I. Heuschkel, A. Schmid, B. Bühler, R. Karande, K. Bühler, *Bioresour. Technol.* **2019**, *282*, 171–178. DOI: https://doi.org/10.1016/j.biortech.2019.02.093

[49] R. Silva-Rocha, E. Martínez-García, B. Calles, M. Chavarría, A. Arce-Rodríguez, A. De Las Heras, A. D. Páez-Espino, G. Durante-Rodríguez, J. Kim, P. I. Nikel, R. Platero, V. De Lorenzo, *Nucleic Acids Res.* **2013**, *41*, 666–675. DOI: https://doi.org/10.1093/nar/gks1119

[50] P. Till, J. Toepel, B. Bühler, R. L. Mach, A. R. Mach-Aigner, *Appl. Microbiol. Biotechnol.* **2020**, *104*, 1977–1991. DOI: https://doi.org/10.1007/s00253-019-10344-w

[51] E. A. Ferreira, C. C. Pacheco, F. Pinto, J. Pereira, P. Lamosa, P. Oliveira, B. Kirov, A. Jaramillo, P. Tamagnini, *Synth. Biol.* **2018**, *3*, ysy014. DOI: https://doi.org/10.1093/synbio/ysy014

[52] J. Zhou, H. Zhang, H. Meng, Y. Zhu, G. Bao, Y. Zhang, Y. Li, Y. Ma, *Sci. Rep.* **2014**, *4*, 4500. DOI: https://doi.org/10.1038/srep04500

[53] K. El Bissati, D. Kirilovsky, *Plant Physiol.* **2001**, *125*, 1988–2000. DOI: https://doi.org/10.1104/pp.125.4.1988

[54] C. Thelwell, N. J. Robinson, J. S. Turner-Cavet, *Proc. Natl. Acad. Sci. U. S. A.* **1998**, *95*, 10728–10733. DOI: https://doi.org/10.1073/pnas.95.18.10728

[55] L. López-Maury, M. García-Domínguez, F. J. Florencio, J. C. Reyes, *Mol. Microbiol.* **2002**, *43*, 247–256. DOI: https://doi.org/10.1046/j.1365-2958.2002.02741.x

[56] B. Blasi, L. Peca, I. Vass, P. B. Kós, *J. Microbiol. Biotechnol.* **2012**, *22*, 166–169. DOI: https://doi.org/10.4014/jmb.1106.06050

[57] L. Peca, P. B. Kós, I. Vass, *Acta Biol. Hung.* **2007**, *58*, 11–22. DOI: https://doi.org/10.1556/ABiol.58.2007.Suppl.2

[58] E. Englund, F. Liang, P. Lindberg, *Sci. Rep.* **2016**, *6*, 36640. DOI: https://doi.org/10.1038/srep36640

[59] C. L. Kelly, G. M. Taylor, A. Hitchcock, A. Torres-Méndez, J. T. Heap, *ACS Synth. Biol.* **2018**, *7*, 1056–1066. DOI: https://doi.org/10.1021/acssynbio.7b00435

[60] A. Behle, P. Saake, A. T. Germann, D. Dienst, I. M. Axmann, *ACS Synth. Biol.* **2020**, *9*, 843–855. DOI: https://doi.org/10.1021/acssynbio.9b00505

[61] S. Tanaka, H. Kojima, S. Takeda, R. Yamanaka, T. Takemura, *Tetrahedron Lett.* **2021**, *77*, 153249. DOI: https://doi.org/10.1016/j.tetlet.2021.153249

[62] S. Rasoul-Amini, E. Fotooh-Abadi, Y. Ghasemi, *J. Appl. Phycol.* **2011**, *23*, 975–981. DOI: https://doi.org/10.1007/s10811-010-9625-4

[63] H. Hamada, Y. Kondo, K. Ishihara, N. Nakajima, H. Hamada, R. Kurihara, T. Hirata, *J. Biosci. Bioeng.* **2003**, *96*, 581–584. DOI: https://doi.org/10.1263/jbb.96.581

[64] K. Shimoda, N. Kubota, H. Hamada, M. Kaji, T. Hirata, *Tetrahedron: Asymmetry* **2004**, *15*, 1677–1679. DOI: https://doi.org/10.1016/j.tetasy.2004.04.024

[65] T. Utsukihara, W. Chai, N. Kato, K. Nakamura, C. A. Horiuchi, *J. Mol. Catal. B: Enzym.* **2004**, *31*, 19–24. DOI: https://doi.org/10.1016/j.molcatb.2004.06.002

[66] M. T. Yazdi, H. Arabi, M. A. Faramarzi, Y. Ghasemi, M. Amini, S. Shokravi, F. A. Mohseni, *Phytochemistry* **2004**, *65*, 2205–2209. DOI: https://doi.org/10.1016/j.phytochem.2004.05.015

[67] R. H. Wijffels, O. Kruse, K. J. Hellingwerf, *Curr. Opin. Biotechnol.* **2013**, *24*, 405–413. DOI: https://doi.org/10.1016/j.copbio.2013.04.004

[68] J. Löwe, A. Siewert, A. C. Scholpp, L. Wobbe, H. Gröger, *Sci. Rep.* **2018**, *8*, 10436. DOI: https://doi.org/10.1038/s41598-018-28755-6

[69] M. Santos-Merino, A. Torrado, G. A. Davis, A. Rottig, T. S. Bibby, D. M. Kramer, D. C. Ducat, *Proc. Natl. Acad. Sci. U. S. A.* **2021**, *118*, e2021523118. DOI: https://doi.org/10.1073/pnas.2021523118

[70] H. M. Woo, *Curr. Opin. Biotechnol.* **2017**, *45*, 1–7. DOI: https://doi.org/10.1016/j.copbio.2016.11.017

[71] R. Stuermer, B. Hauer, M. Hall, K. Faber, *Curr. Opin. Chem. Biol.* **2007**, *11*, 203–213. DOI: https://doi.org/10.1016/j.cbpa.2007.02.025

[72] M. D. Patil, G. Grogan, A. Bommarius, H. Yun, *ACS Catal.* **2018**, *8*, 10985–11015. DOI: https://doi.org/10.1021/acscatal.8b02924

[73] S. Schmidt, C. Scherkus, J. Muschiol, U. Menyes, T. Winkler, W. Hummel, H. Gröger, A. Liese, H. G. Herz, U. T. Bornscheuer, *Angew. Chem., Int. Ed.* **2015**, *54*, 2784–2787. DOI: https://doi.org/10.1002/anie.201410633

[74] J. M. Woo, E. Y. Jeon, E. J. Seo, J. H. Seo, D. Y. Lee, Y. J. Yeon, J. B. Park, *Sci. Rep.* **2018**, *8*, 10280. DOI: https://doi.org/10.1038/s41598-018-28575-8

[75] L. Nikkanen, D. Solymosi, M. Jokel, Y. Allahverdiyeva, *Physiol. Plant.* **2021**, *173*, 514–525. DOI: https://doi.org/10.1111/ppl.13404

[76] Y. Allahverdiyeva, H. Mustila, M. Ermakova, L. Bersanini, P. Richaud, G. Ajlani, N. Battchikova, L. Cournac, E. M. Aro, *Proc. Natl. Acad. Sci. U. S. A.* **2013**, *110*, 4111–4116. DOI: https://doi.org/10.1073/pnas.1221194110

[77] P. Tamagnini, E. Leitão, P. Oliveira, D. Ferreira, F. Pinto, D. J. Harris, T. Heidorn, P. Lindblad, *FEMS Microbiol. Rev.* **2007**, *31*, 692–720. DOI: https://doi.org/10.1111/j.1574-6976.2007.00085.x

[78] G. Shimakawa, C. Miyake, *Photosynth. Res.* **2018**, *137*, 241–250. DOI: https://doi.org/10.1007/s11120-018-0495-y

[79] A. Torrado, H. M. Connabeer, A. Ro, N. Pratt, A. J. Baylay, M. J. Terry, C. M. Moore, T. S. Bibby, *Plant Physiol.* **2022**, *189*, 2554–2566. DOI: https://doi.org/10.1093/plphys/kiac203

[80] A. Berepiki, J. R. Gittins, C. M. Moore, T. S. Bibby, *Synth. Biol.* **2018**, *3*, ysy009. DOI: https://doi.org/10.1093/synbio/ysy009

[81] A. J. J. Straathof, S. Panke, A. Schmid, *Curr. Opin. Biotechnol.* **2002**, *13*, 548–556. DOI: https://doi.org/10.1016/S0958-1669(02)00360-9

[82] G. C. Dismukes, D. Carrieri, N. Bennette, G. M. Ananyev, M. C. Posewitz, *Curr. Opin. Biotechnol.* **2008**, *19*, 235–240. DOI: https://doi.org/10.1016/j.copbio.2008.05.007

[83] T. J. Johnson, S. Katuwal, G. A. Anderson, L. Gu, R. Zhou, W. R. Gibbons, *Biotechnol. Prog.* **2018**, *34*, 811–827. DOI: https://doi.org/10.1002/btpr.2628

[84] J. Jodlbauer, T. Rohr, O. Spadiut, M. D. Mihovilovic, F. Rudroff, *Trends Biotechnol.* **2021**, *39*, 875–889. DOI: https://doi.org/10.1016/j.tibtech.2020.12.009

[85] S. N. Kosourov, M. Seibert, *Biotechnol. Bioeng.* **2009**, *102*, 50–58. DOI: https://doi.org/10.1002/bit.22050

[86] T. V. Laurinavichene, A. S. Fedorov, M. L. Ghirardi, M. Seibert, A. A. Tsygankov, *Int. J. Hydrogen Energy* **2006**, *31*, 659–667. DOI: https://doi.org/10.1016/j.ijhydene.2005.05.002

[87] J. J. Hahn, M. L. Ghirardi, W. A. Jacoby, *Biochem. Eng. J.* **2007**, *37*, 75–79. DOI: https://doi.org/10.1016/j.bej.2007.03.010

[88] V. Rissanen, S. Vajravel, S. Kosourov, S. Arola, E. Kontturi, Y. Allahverdiyeva, T. Tammelin, *Green Chem.* **2021**, *23*, 3715–3724. DOI: https://doi.org/10.1039/d1gc00502b

[89] S. Vajravel, S. Sirin, S. Kosourov, Y. Allahverdiyeva, *Green Chem.* **2020**, *22*, 6404–6414. DOI: https://doi.org/10.1039/d0gc01830a

[90] M. Bozan, A. Schmid, K. Bühler, *Biofilm* **2022**, *4*, 100073. DOI: https://doi.org/10.1016/j.bioflm.2022.100073

[91] T. Saito, Y. Nishiyama, J. L. Putaux, M. Vignon, A. Isogai, *Biomacromolecules* **2006**, *7*, 1687–1691. DOI: https://doi.org/10.1021/bm060154s

[92] C. Posten, *Eng. Life Sci.* **2009**, *9*, 165–177. DOI: https://doi.org/10.1002/elsc.200900003

[93] S. N. Chanquia, A. Valotta, H. Gruber-Woelfler, S. Kara, *Front. Catal.* **2022**, *1*, 816538. DOI: https://doi.org/10.3389/fctls.2021.816538
[94] M. Heining, A. Sutor, S. C. Stute, C. P. Lindenberger, R. Buchholz, *J. Appl. Phycol.* **2015**, *27*, 59–66.
[95] A. K. Sadvakasova, B. D. Kossalbayev, B. K. Zayadan, D. K. Kirbayeva, S. Alwasel, S. I. Allakhverdiev, *World J. Microbiol. Biotechnol.* **2021**, *37 (8)*, 140. DOI: https://doi.org/10.1007/s11274-021-03107-1
[96] P. Farrokh, M. Sheikhpour, A. Kasaeian, H. Asadi, R. Bavandi, *Biotechnol. Prog.* **2019**, *35 (5)*, e2835. DOI: https://doi.org/10.1002/btpr.2835
[97] N. K. Mund, Y. Liu, S. Chen, *Fuel* **2022**, *322*, 124117. DOI: https://doi.org/10.1016/j.fuel.2022.124117

